Comput Mech (2007) 39:309–322
DOI 10.1007/s00466-006-0029-x

ORIGINAL PAPER

A co-rotational formulation for 3D beam element using vectorial rotational variables

Z. X. Li

Received: 14 April 2005 / Accepted: 23 December 2005 / Published online: 31 August 2006

Abstract Based on a co-rotational framework, a 3-noded iso-parametric element formulation of 3D beam was presented, which was used for accurate modelling of frame structures with large displacements and large rotations. Firstly, a co-rotational framework was fixed at the internal node of the element, it translates and rotates with the node rigidly; then, vectorial rotational variables were defined, they are three smaller components of the cross-sectional principal vectors at each node, sometimes they represent different components of the cross-sectional principal vectors in incremental solution procedure so as to avoid the occurrence of ill-conditioned tangent stiffness matrix; thereafter, the internal force vector and tangent stiffness matrix in local system was derived from the strain energy of the element as its first partial derivative and second partial derivative with respect to local variables, respectively, and a symmetric tangent stiffness matrix was achieved; finally, several examples were analysed to illustrate the reliability and accuracy of this procedure.

Keywords Co-rotational procedure · Vectorial rotational variable · Large rotation · Large displacement · 3D beam element

This work is supported by National Natural Science Foundation of China (50408022), and the Scientific Research Foundation for the Returned Overseas Chinese Scholars, State Education Ministry and Zhejiang Province.

Z. X. Li (✉)
Department of Civil Engineering,
Zhejiang University,
Hangzhou 310027, China
e-mail: lizx19993@zju.edu.cn

1 Introduction

Developing an efficient beam element formulation for large displacement analysis of frame structures has been an issue of many researchers (Crisfield 1996, Hsiao et al. 1987). There already exist various formulations to meet this requirement, Hsiao et al. (1987) had divided them into three categories: Total Lagrangian formulation (Bathe and Bolourchi 1979, Kwak et al. 2001, Pai et al. 2000, Schulz and Filippou 2001). Updated Lagrangian formulation (Bathe and Bolourchi 1979, Cardona and Geradin 1988, Chen and Blandford 1991, Misra et al. 2000, Teh and Clarke 1999) and co-rotational formulation (Battini and Pacoste 2002, Crisfield 1990, Crisfield and Moita 1996, Hsiao et al. 1987, Hsiao and Lin 2000a, Teh and Clarke 1998), certainly, there also exist some mixed type formulations of them (Jiang and Chernuka 1994, Hsiao and Lin 2000b, Lin and Hsiao 2001). In addition, Simo and Vu-Quoc developed a class of geometrically-exact beam formulation, this formulation demonstrates its computational efficiency in large displacement analyses of frame structures and benefit in solving dynamic problems of flexible beam or beams system subject to large overall motions (Simo and Vu-Quoc 1986a,b, 1988, 1991, Vu-Quoc and Deng 1995, Vu-Quoc and Ebcioglu 1995, 1996, Vu-Quoc and Simo 1987). For convenience, these formulations can also be classified into two groups: formulations with asymmetric element tangent stiffness matrices and formulations with symmetric element tangent stiffness matrices. Due to the non-commutativity of spatial rotations, most co-rotational formulations belong to the first group, and the geometrically-exact beam formulation proposed by Simo and Vu-Quoc also falls into this category (Simo and Vu-Quoc 1986a,b, 1988, 1991, Vu-Quoc and Deng 1995, Vu-Quoc and Ebcioglu 1995, 1996, Vu-Quoc and Simo 1987). For an asymmetric tangent stiffness matrix, more storage is occupied so as to store all its components. Simo and Vu-Quoc (1986c) denoted that in a conservative system, although their developing tangent stiffness matrix is always asymmetric, it will become symmetric once the incremental loading process arrives at an equilibrium level, Crisfield and his co-worker (Crisfield 1990, 1996, Crisfield and Moita 1996) had also found this phenomenon, so they symmetrized element tangent stiffness matrix by excluding the non-symmetric term (Simo and Vu-Quoc 1986c, Crisfield 1990, 1996, Crisfield and Moita 1996). This treatment can improve the computational efficiency greatly. Simo (1992) presented a rigorous justification for the symmetrization of non-symmetric tangent stiffness matrix. Simo (1992) and Crisfield (1996) also predicted that a symmetric tangent stiffness matrix in the co-rotational framework could be achieved if a certain set of additive rotational variables were adopted.

Up to now, numerous theoretical models of beams have been developed and applied to various practical circumstances. No single theory has proven to be general and comprehensive enough for the entire range of applications. Some beam formulations address better performance over certain class of physical problems with greater accuracy and efficiency rather than their generality, while, other models tend to a wider range of practical engineering problems, and the accuracy of the formulations has been somewhat sacrificed. In this paper, the author defined a set of vectorial rotational variables and developed an advanced co-rotational formulation for 3D beam element. In contrast with other existing beam element formulations for large displacement and large rotation analysis of frame structures, this formulation has several advantages: (1) all the variables are additive in an incremental solution procedure, this renders great simplification in updating vectorial rotational variables in incremental loading; (2) a quite simple relationship is established between the local variables and the global variables, and the transformation matrix can be derived from this relationship conveniently; (3) symmetric tangent stiffness matrices are achieved both in local system and global system; (4) total variables are used in calculating tangent stiffness matrix in local system and global system, this ensures the accuracy and reliability of beam element formulation. Considering the merits of the proposed co-rotational procedure and vectorial rotational variables, the author and his co-worker (Izzuddin and LI 2004, Li and Izzuddin 2005) have also extended them to 2D beam element, curved shell element, multi-layered tube-like beam element, laminated curved shell element and several super-elements consisting of multiple tube-like beam and shell elements in bionic structural modelling of dragonfly's wing.

2 Description of the co-rotational framework

In this beam element formulation, several basic assumptions were adopted: (1) all elements are straight at the initial configuration; (2) the shape of the cross-section does not distort with element deforming; (3) restrained warping effects are ignored. Certainly, this co-rotational procedure and vectorial rotational variables can also be easily extended to solve some complicated beam or shell problems, such as open cross-section beams, curved beam, multi-layered composite beam and laminated curved shell element etc.

Local coordinate system and global coordinate system are illustrated in Fig. 1, both of them are Cartesian coordinate systems, where the local coordinate system is fixed at the internal node of element, and translates and rotates with the element rigid-body translation and rotation, but does not deform with the element.

In order to define the initial orientation of the local coordinate axes, an auxiliary node is prescribed, which is located in one of the symmetry plane of the element (see Point A in Fig. 1). Vectors $\mathbf{v}_{120}$ and $\mathbf{v}_{3A0}$ are calculated from,

$$\mathbf{v}_{120} = \mathbf{X}_{20} - \mathbf{X}_{10} \quad \mathbf{v}_{3A0} = \mathbf{X}_{A0} - \mathbf{X}_{30}$$

where, $\mathbf{X}_{i0} (i = 1, 2, 3, A)$ is the global coordinates of Node i, then the orientation vectors of local axes are defined as,

$$\mathbf{e}_{x0} = \frac{\mathbf{v}_{120}}{|\mathbf{v}_{120}|} \quad \mathbf{e}_{z0} = \frac{\mathbf{v}_{120} \times \mathbf{v}_{3A0}}{|\mathbf{v}_{120} \times \mathbf{v}_{3A0}|} \quad \mathbf{e}_{y0} = \mathbf{e}_{z0} \times \mathbf{e}_{x0}$$

where, $\mathbf{e}_{x0}, \mathbf{e}_{y0}, \mathbf{e}_{z0}$ (see Fig. 1) are the normalized orientation vectors of x-axis, y-axis and z-axis in global coordinate system, respectively.

The orientation vectors $\mathbf{e}_{ix}, \mathbf{e}_{iy}, \mathbf{e}_{iz}$ of Node i at the deformed configuration are calculated from the rotational variables directly in incremental solution procedure. In particular, at Node 3 (the internal node), $\mathbf{e}_{3x}, \mathbf{e}_{3y}, \mathbf{e}_{3z}$ are coincident with the orientations of local coordinate axes,

$$\mathbf{e}_{3x} = \mathbf{e}_x \quad \mathbf{e}_{3y} = \mathbf{e}_y \quad \mathbf{e}_{3z} = \mathbf{e}_z$$

and at the initial configuration,

$$\mathbf{e}_{3x0} = \mathbf{e}_{x0} \quad \mathbf{e}_{3y0} = \mathbf{e}_{y0} \quad \mathbf{e}_{3z0} = \mathbf{e}_{z0}$$

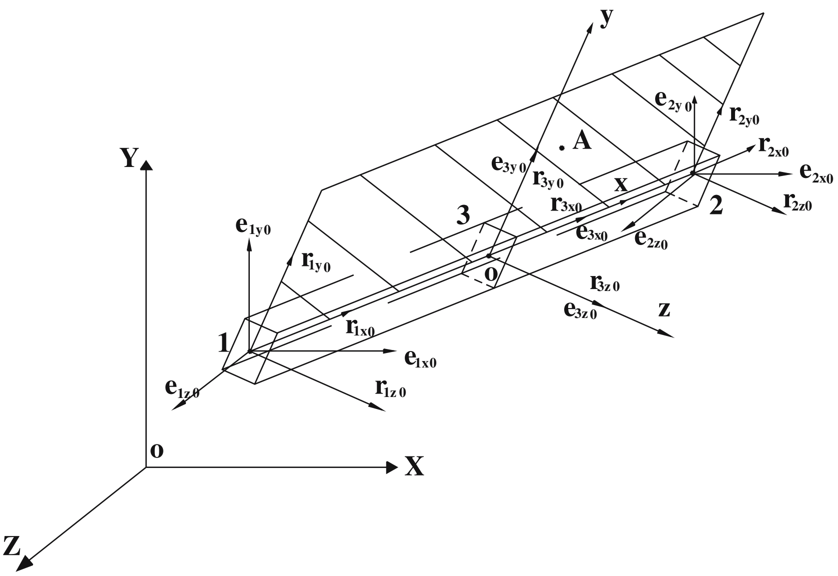

Fig. 1 Definition of the initial configuration

however, the initial orientation vectors of two end nodes are defined as

$$\mathbf{e}_{ix0} = \{1, 0, 0\}^{\mathrm{T}} \quad \mathbf{e}_{iy0} = \{0, 1, 0\}^{\mathrm{T}}$$
$$\mathbf{e}_{iz0} = \{0, 0, 1\}^{\mathrm{T}} \quad i = 1, 2$$

In global coordinate system, there are 18 degree of freedoms per element, and each node six freedoms,

$$\mathbf{u}_G = \{U_1\ V_1\ W_1\ e_{1y,n_1}\ e_{1y,m_1}\ e_{1z,n_1},\ \ldots,\ U_3\ V_3\ W_3\ e_{3y,n_3}\ e_{3y,m_3}\ e_{3z,n_3}\}^{\mathrm{T}}$$

where, U_i, V_i and W_i are the displacements of Node i, e_{iy,n_i}, e_{iy,m_i} and e_{iz,n_i} are the vectorial rotational variables, they are three smaller components of $\mathbf{e}_{iy}$ and $\mathbf{e}_{iz}$. This definition can eliminate the possibility of the denominators approaching to 'zero' in the partial derivatives of the rest components of $\mathbf{e}_{iy}$ and $\mathbf{e}_{iz}$ with respect to e_{iy,n_i}, e_{iy,m_i} and e_{iz,n_i} [referred to Eqs. (2) and (3)], accordingly, avoid the occurrence of ill-conditioned tangent stiffness matrix in global system.

In local coordinate system, there are 12 freedoms per element, and each end node 6 degree of freedoms,

$$\mathbf{u}_L = \{u_1 v_1\ w_1\ r_{1y,n_1}\ r_{1y,m_1}\ r_{1z,n_1}\ u_2\ v_2\ w_2\ r_{2y,n_2}\ r_{2y,m_2}\ r_{2z,n_2}\}^{\mathrm{T}}$$

where, u_i, v_i, w_i are the local displacements of Node i, and r_{iy,n_i}, r_{iy,m_i} and r_{iz,n_i} are the local vectorial rotational variables, which are three smaller components of $\mathbf{r}_{iy}$ and $\mathbf{r}_{iz}$. This definition can avoid the occurrence of ill-conditioned tangent stiffness matrix in local system.

Considering that $\mathbf{e}_{iy}$ and $\mathbf{e}_{iz}$ are always orthogonal $\mathbf{e}_{iy}^{\mathrm{T}}\mathbf{e}_{iz} = 0$, and both of them are unit vectors, the rest components of $\mathbf{e}_{iy}$ and $\mathbf{e}_{iz}$ can be calculated from the rotational variables e_{iy,n_i}, e_{iy,m_i} and e_{iz,n_i}according to the following equations,

$$e_{iy,l}e_{iz,l} + e_{iy,m}e_{iz,m} + e_{iy,n}e_{iz,n} = 0 \tag{1a}$$
$$e_{iy,l}^2 + e_{iy,m}^2 + e_{iy,n}^2 = 1 \tag{1b}$$
$$e_{iz,l}^2 + e_{iz,m}^2 + e_{iz,n}^2 = 1 \tag{1c}$$

Firstly, assumed that $|e_{iy,l}| \geq |e_{iy,m}|$, $|e_{iy,l}| \geq |e_{iy,n}|$ ($l, m, n \in \{1, 2, 3\}$, and $l \neq m \neq n$) at the end of the current incremental loading or iterating step:

Case 1 If $|e_{iz,l}| \geq |e_{iz,m}|$ and $|e_{iz,l}| \geq |e_{iz,n}|$, then three rotational variables at the next incremental loading or iterating step are $e_{iy,n}, e_{iy,m}, e_{iz,n}$, where $\{n\ m\ l\}$ are the cyclic permutations of $\{1\ 2\ 3\}$, according to Eq. (1), other components of $\mathbf{e}_{iy}$ and $\mathbf{e}_{iz}$ are calculated from these rotational variables as,

$$e_{iy,l} = s_1\sqrt{1 - e_{iy,n}^2 - e_{iy,m}^2} \tag{2a}$$
$$e_{iz,m} = \frac{-e_{iy,m}e_{iy,n}e_{iz,n} + s_2 e_{iy,l}\sqrt{1 - e_{iy,n}^2 - e_{iz,n}^2}}{1 - e_{iy,n}^2} \tag{2b}$$
$$e_{iz,l} = s_3\sqrt{1 - e_{iz,m}^2 - e_{iz,n}^2} \tag{2c}$$

where, s_1, s_3 are the sign flags of $e_{iy,l}$ and $e_{iz,l}$ at the start of the incremental loading or iterating step, respectively, they are one of the numeric values of 1 or –1, s_2 is also such a constant, and it is conditioned on $\mathbf{e}_{iy}^{\mathrm{T}}\mathbf{e}_{iz} = 0$. Note that n, m, l may have different values at different node or at different incremental loading or iterating step.

Case 2 If $|e_{iz,m}| \geq |e_{iz,l}|$ and $|e_{iz,m}| \geq |e_{iz,n}|$ at the end of the current incremental loading or iterating step, then three rotational variables are defined as $e_{iy,n}, e_{iy,m}, e_{iz,n}$, according to Eq. (1), other components of $\mathbf{e}_{iy}$ and $\mathbf{e}_{iz}$ are calculated from them as,

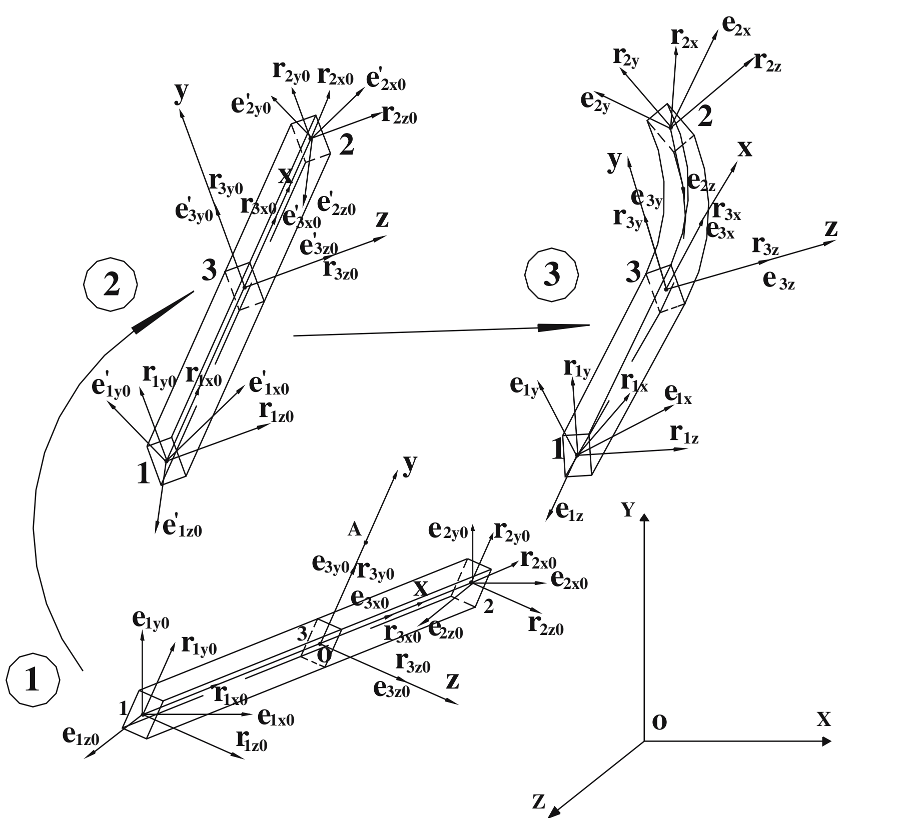

Fig. 2 Diagram of the co-rotational framework

$$e_{iy,l} = s_1\sqrt{1 - e_{iy,n}^2 - e_{iy,m}^2} \tag{3a}$$

$$e_{iz,l} = \frac{-s_1\sqrt{1-e_{iy,m}^2-e_{iy,n}^2}\,e_{iy,n}e_{iz,n}+s_2 e_{iy,m}\sqrt{1-e_{iy,n}^2-e_{iz,n}^2}}{1-e_{iy,n}^2} \tag{3b}$$

$$e_{iz,m} = s_3\sqrt{1 - e_{iz,n}^2 - e_{iz,l}^2} \tag{3c}$$

where, s_1, s_2, s_3 are the same kind of constants as those in case 1.

Vector $\mathbf{e}_{ix}$ is the cross-product of vectors $\mathbf{e}_{iy}$ and $\mathbf{e}_{iz}$,

$$\mathbf{e}_{ix} = \mathbf{e}_{iy} \times \mathbf{e}_{iz} \tag{4}$$

The definition of local vectorial rotational variables r_{iy,n_i}, r_{iy,m_i} and r_{iz,n_i} (they are three smaller components of $\mathbf{r}_{iy}$ and $\mathbf{r}_{iz}$) follows the same route as that of global vectorial rotational variables (e_{iy,n_i}, e_{iy,m_i} and e_{iz,n_i} are three smaller components of $\mathbf{e}_{iy}$ and $\mathbf{e}_{iz}$).

Rigid-body motion contributes nothing to strain, so it is excluded in advance so as to achieve an element-independent co-rotational formulation. In Fig. 2, (1) denotes the initial configuration; (3) represents the current configuration. From (1) to (3), the element experiences both rigid-body motion and pure deformation. (2) is an intermediate configuration between (1) and (3). From (1) to (2), the element experiences pure rigid-body motion, and from (2) to (3), it suffers pure deformation. In the co-rotational framework presented in Fig.2, the process from (1) to (2) is excluded, and only the process from (2) to (3) is considered, where, (2) is treated as a pseudo initial configuration of (3), so the relationships of local variables and global variables are given as,

$$\mathbf{t}_i = \mathbf{R}(\mathbf{d}_i - \mathbf{d}_3 + \mathbf{v}_{i0}) - \mathbf{R}_0\mathbf{v}_{i0} \tag{5a}$$

$$\mathbf{r}_{iy} = \mathbf{R}\mathbf{R}_i^{\mathrm{T}}\mathbf{e}_{y0} \tag{5b}$$

$$\mathbf{r}_{iz} = \mathbf{R}\mathbf{R}_i^{\mathrm{T}}\mathbf{e}_{z0} \tag{5c}$$

where, $\mathbf{t}_i = \begin{Bmatrix} u_i \\ v_i \\ w_i \end{Bmatrix}$, $\mathrm{R}_0 = \begin{bmatrix} \mathbf{e}_{x0}^{\mathrm{T}} \\ \mathbf{e}_{y0}^{\mathrm{T}} \\ \mathbf{e}_{z0}^{\mathrm{T}} \end{bmatrix}$, $\mathrm{R} = \begin{bmatrix} \mathbf{e}_{x}^{\mathrm{T}} \\ \mathbf{e}_{y}^{\mathrm{T}} \\ \mathbf{e}_{z}^{\mathrm{T}} \end{bmatrix}$, $\mathrm{R}_i = \begin{bmatrix} \mathbf{e}_{ix}^{\mathrm{T}} \\ \mathbf{e}_{iy}^{\mathrm{T}} \\ \mathbf{e}_{iz}^{\mathrm{T}} \end{bmatrix}$ $(i = 1,\ 2)$. At the right side of Eq. (5a), the first term is the local coordinates of Node i at the deformed configuration, while, the second term is its initial local coordinates. At the right side of Eq. (5b,5c), $\hat{\mathbf{e}}_{iy} = \mathbf{R}_i^{\mathrm{T}}\mathbf{e}_{y0}$ and $\hat{\mathbf{e}}_{iz} = \mathbf{R}_i^{\mathrm{T}}\mathbf{e}_{z0}$ are the cross-sectional principal vectors of Node i at the deformed configuration (they are coincident with $\mathbf{e}_{y0}$ and $\mathbf{e}_{z0}$ at undeformed configuration for a straight beam element, and the nodal orientation matrix $\mathbf{R}_{i0}$ at initial configuration is a unit matrix, while, at the deformed configuration, it becomes $\mathbf{R}_i$. Note that $\mathbf{R}_i\hat{\mathbf{e}}_{iy} = \mathbf{R}_{i0}\mathbf{e}_{y0}$ and $\mathbf{R}_i\hat{\mathbf{e}}_{iz} = \mathbf{R}_{i0}\mathbf{e}_{z0}$, accordingly, $\hat{\mathbf{e}}_{iy} = \mathbf{R}_i^{\mathrm{T}}\mathbf{e}_{y0}$ and $\hat{\mathbf{e}}_{iz} = \mathbf{R}_i^{\mathrm{T}}\mathbf{e}_{z0}$). $\mathbf{v}_{i0}$ is the relative vector from Node 3 to Node i at the initial configuration, it is calculated from,

$$\mathbf{v}_{i0} = \mathbf{X}_{i0} - \mathbf{X}_{30} \quad i = 1, 2 \tag{6}$$

Especially, at the internal node, $\mathbf{t}_3 = \{0, 0, 0\}^{\mathrm{T}}$, $\mathbf{r}_{3x0} = \mathbf{r}_{3x} = \{1, 0, 0\}^{\mathrm{T}}$, $\mathbf{r}_{3y0} = \mathbf{r}_{3y} = \{0, 1, 0\}^{\mathrm{T}}$, $\mathbf{r}_{3z0} = \mathbf{r}_{3z} = \{0, 0, 1\}^{\mathrm{T}}$.

3 Kinematics of 3-noded iso-parametric beam element

For this 3-noded iso-parametric beam element, Lagrangian interpolation functions are introduced to describe the coordinates, displacements and vectorial rotations at any point of element in local coordinate system.

The local coordinates at any point of element are depicted as

$$\mathbf{x} = \sum_{i=1}^{3} h_i(\xi)\left(\mathbf{x}_{i0} + y_l \mathbf{r}_{iy0} + z_l \mathbf{r}_{iz0}\right) \tag{7}$$

where, $\mathbf{x} = \{x, y, z\}^{\mathrm{T}}$; $h_i(\xi)$ is Lagrangian interpolation function at Node i; $\mathbf{x}_{i0} = \{x_{i0}, y_{i0}, z_{i0}\}^{\mathrm{T}}$ are the local coordinates of Node i; y_l and z_l are the relative coordinates of a point to the central line of element along its two cross-sectional principal vectors, respectively, in the proposed formulation, $y_l = y$, $z_l = z$.

The displacements at any point of element can be expressed as,

$$\mathbf{u} = \sum_{i=1}^{3} h_i(\xi)\left[\mathbf{t}_i + y_l\left(\mathbf{r}_{iy} - \mathbf{r}_{iy0}\right) + z_l\left(\mathbf{r}_{iz} - \mathbf{r}_{iz0}\right)\right] \tag{8}$$

Considering the possibility of large displacements and large rotations, Green strain measure is introduced to describe the strain–displacement relationship of this beam element formulation,

$$\varepsilon = \begin{Bmatrix} \varepsilon_{xx} \\ \gamma_{xy} \\ \gamma_{xz} \end{Bmatrix} = \begin{Bmatrix} \frac{1}{2}\left[\frac{\partial(\mathbf{u}+\mathbf{x})}{\partial x}\frac{\partial(\mathbf{u}+\mathbf{x})}{\partial x} - \frac{\partial \mathbf{x}}{\partial x}\frac{\partial \mathbf{x}}{\partial x}\right] \\ \frac{\partial(\mathbf{u}+\mathbf{x})}{\partial x}\frac{\partial(\mathbf{u}+\mathbf{x})}{\partial y} - \frac{\partial \mathbf{x}}{\partial x}\frac{\partial \mathbf{x}}{\partial y} \\ \frac{\partial(\mathbf{u}+\mathbf{x})}{\partial x}\frac{\partial(\mathbf{u}+\mathbf{x})}{\partial z} - \frac{\partial \mathbf{x}}{\partial x}\frac{\partial \mathbf{x}}{\partial z} \end{Bmatrix} \tag{9}$$

For convenience, Eq. (9) is rewritten as,

$$\varepsilon = \varepsilon^{(0)} + y_l\varepsilon^{(1)} + z_l\varepsilon^{(2)} + y_l z_l\varepsilon^{(3)} + y_l^2\varepsilon^{(4)} + z_l^2\varepsilon^{(5)}$$

where,

$$\varepsilon^{(0)} = \begin{Bmatrix} \frac{1}{2}\frac{\partial \mathbf{u}_0}{\partial x}\frac{\partial \mathbf{u}_0}{\partial x} + \frac{\partial \mathbf{u}_0}{\partial x}\frac{\partial \mathbf{x}}{\partial x} \\ \frac{\partial \mathbf{u}_0}{\partial x}\mathbf{r}_y + \frac{\partial \mathbf{x}}{\partial x}\left(\mathbf{r}_y - \mathbf{r}_{y0}\right) \\ \frac{\partial \mathbf{u}_0}{\partial x}\mathbf{r}_z + \frac{\partial \mathbf{x}}{\partial x}\left(\mathbf{r}_z - \mathbf{r}_{z0}\right) \end{Bmatrix}$$

$$\varepsilon^{(1)} = \begin{Bmatrix} \frac{1}{2}\frac{\partial \mathbf{u}_0}{\partial x}\frac{\partial \mathbf{r}_y}{\partial x} + \frac{\partial \mathbf{x}}{\partial x}\frac{\partial(\mathbf{r}_y - \mathbf{r}_{y0})}{\partial x} \\ \frac{\partial \mathbf{r}_y}{\partial x}\mathbf{r}_y - \frac{\partial \mathbf{r}_{y0}}{\partial x}\mathbf{r}_{y0} \\ \frac{\partial \mathbf{r}_y}{\partial x}\mathbf{r}_z - \frac{\partial \mathbf{r}_{y0}}{\partial x}\mathbf{r}_{z0} \end{Bmatrix}$$

$$\varepsilon^{(2)} = \begin{Bmatrix} \frac{1}{2}\frac{\partial \mathbf{u}_0}{\partial x}\frac{\partial \mathbf{r}_z}{\partial x} + \frac{\partial \mathbf{x}}{\partial x}\frac{\partial(\mathbf{r}_z - \mathbf{r}_{z0})}{\partial x} \\ \frac{\partial \mathbf{r}_z}{\partial x}\mathbf{r}_y - \frac{\partial \mathbf{r}_{z0}}{\partial x}\mathbf{r}_{y0} \\ \frac{\partial \mathbf{r}_z}{\partial x}\mathbf{r}_z - \frac{\partial \mathbf{r}_{z0}}{\partial x}\mathbf{r}_{z0} \end{Bmatrix}$$

$$\varepsilon^{(3)} = \begin{Bmatrix} \frac{1}{2}\frac{\partial \mathbf{r}_y}{\partial x}\frac{\partial \mathbf{r}_z}{\partial x} - \frac{\partial \mathbf{r}_{y0}}{\partial x}\frac{\partial \mathbf{r}_{z0}}{\partial x} \\ 0 \\ 0 \end{Bmatrix}$$

$$\varepsilon^{(4)} = \begin{Bmatrix} \frac{1}{2}\left(\frac{\partial \mathbf{r}_y}{\partial x}\frac{\partial \mathbf{r}_y}{\partial x} - \frac{\partial \mathbf{r}_{y0}}{\partial x}\frac{\partial \mathbf{r}_{y0}}{\partial x}\right) \\ 0 \\ 0 \end{Bmatrix}$$

$$\varepsilon^{(5)} = \begin{Bmatrix} \frac{1}{2}\left(\frac{\partial \mathbf{r}_z}{\partial x}\frac{\partial \mathbf{r}_z}{\partial x} - \frac{\partial \mathbf{r}_{z0}}{\partial x}\frac{\partial \mathbf{r}_{z0}}{\partial x}\right) \\ 0 \\ 0 \end{Bmatrix}$$

and $\mathbf{u}_0 = \sum_{i=1}^{3} h_i(\xi)\,\mathbf{t}_i; \mathbf{r}_y = \sum_{i=1}^{3} h_i(\xi)\,\mathbf{r}_{iy}; \mathbf{r}_{y0} = \sum_{i=1}^{3} h_i(\xi)\,\mathbf{r}_{iy0}; \mathbf{r}_z = \sum_{i=1}^{3} h_i(\xi)\,\mathbf{r}_{iz}; \mathbf{r}_{z0} = \sum_{i=1}^{3} h_i(\xi)\,\mathbf{r}_{iz0}$; $\frac{\partial}{\partial x} = \frac{\partial}{\partial \xi}/\sum_{i=1}^{3} h_i'(\xi)x_{i0}$, the prime appended above and to the right of $h_i(\xi)$ represents its first derivative with respect to ξ.

4 Definition of element tangent stiffness matrix

The strain energy of element can be calculated as below,

$$U = \int_V \frac{1}{2}\varepsilon^{\mathrm{T}}\mathbf{D}\varepsilon \mathrm{d}V \tag{10}$$

where, $\mathbf{D}$ is the elastic constant matrix, $\mathbf{D} = \begin{bmatrix} E & 0 & 0 \\ 0 & k_0 G & 0 \\ 0 & 0 & k_0 G \end{bmatrix}$; E and G are the elastic modulus and shear modulus, respectively; k_0 is the shear factor of cross-section; V the volume of element.

The internal force vector in local system is the first derivatives of the strain energy with respect to local variables, it is calculated from

$$\mathbf{f} = \frac{\partial U}{\partial \mathbf{u}_L} = \int_V \mathbf{B}^{\mathrm{T}}\mathbf{D}\varepsilon \mathrm{d}V \tag{11}$$

where,

$$\mathbf{B} = \frac{\partial \varepsilon}{\partial \mathbf{u}_L} = \frac{\partial \varepsilon^{(0)}}{\partial \mathbf{u}_L} + y_l \frac{\partial \varepsilon^{(1)}}{\partial \mathbf{u}_L} + z_l \frac{\partial \varepsilon^{(2)}}{\partial \mathbf{u}_L} + y_l z_l \frac{\partial \varepsilon^{(3)}}{\partial \mathbf{u}_L} + y_l^2 \frac{\partial \varepsilon^{(4)}}{\partial \mathbf{u}_L} + z_l^2 \frac{\partial \varepsilon^{(5)}}{\partial \mathbf{u}_L}$$
$$= \mathbf{B}^{(0)} + y_l \mathbf{B}^{(1)} + z_l \mathbf{B}^{(2)} + y_l z_l \mathbf{B}^{(3)} + y_l^2 \mathbf{B}^{(4)} + z_l^2 \mathbf{B}^{(5)}$$

Eq. (11) can be rewritten as

$$\mathbf{f} = \int_L \left(\int_A \mathbf{B}^{\mathrm{T}} \mathbf{D} \varepsilon \mathrm{d}A \right) \mathrm{d}x$$
$$= \int_L (\mathbf{a}_0 A + \mathbf{a}_1 S_y + \mathbf{a}_2 S_z + \mathbf{a}_3 S_{yz} + \mathbf{a}_4 I_y + \mathbf{a}_5 I_z + \mathbf{a}_6 S_{wyz} + \mathbf{a}_7 S_{wzy} + \mathbf{a}_8 I_{wyz} + \mathbf{a}_9 I_{wy} + \mathbf{a}_{10} I_{wz}) \, \mathrm{d}x$$

where, A and L are the cross-sectional area and length of beam element, respectively; $A = \int_A \mathrm{d}A$; $S_y = \int_A y_l \mathrm{d}A$; $S_z = \int_A z_l \mathrm{d}A$; $S_{yz} = \int_A y_l z_l \mathrm{d}A$; $I_y = \int_A y_l^2 \mathrm{d}A$; $I_z = \int_A z_l^2 \mathrm{d}A$; $S_{wyz} = \int_A y_l^2 z_l \mathrm{d}A$; $S_{wzy} = \int_A z_l^2 y_l \mathrm{d}A$; $I_{wyz} = \int_A y_l^2 z_l^2 \mathrm{d}A$; $I_{wy} = \int_A y_l^4 \mathrm{d}A$; $I_{wz} = \int_A z_l^4 \mathrm{d}A$, for a beam element with bisymmetric cross-section, $S_y = S_z = S_{yz} = S_{wyz} = S_{wzy} = 0$; $\mathbf{a}_0 \sim \mathbf{a}_{10}$ can be calculated as below,

$$\mathbf{a}_0 = \mathbf{B}^{(0)^{\mathrm{T}}} \mathbf{D} \varepsilon^{(0)}$$
$$\mathbf{a}_1 = \mathbf{B}^{(1)^{\mathrm{T}}} \mathbf{D} \varepsilon^{(0)} + \mathbf{B}^{(0)^{\mathrm{T}}} \mathbf{D} \varepsilon^{(1)}$$
$$\mathbf{a}_2 = \mathbf{B}^{(2)^{\mathrm{T}}} \mathbf{D} \varepsilon^{(0)} + \mathbf{B}^{(0)^{\mathrm{T}}} \mathbf{D} \varepsilon^{(2)}$$
$$\mathbf{a}_3 = \mathbf{B}^{(3)^{\mathrm{T}}} \mathbf{D} \varepsilon^{(0)} + \mathbf{B}^{(0)^{\mathrm{T}}} \mathbf{D} \varepsilon^{(3)} + \mathbf{B}^{(2)^{\mathrm{T}}} \mathbf{D} \varepsilon^{(1)} + \mathbf{B}^{(1)^{\mathrm{T}}} \mathbf{D} \varepsilon^{(2)}$$
$$\mathbf{a}_4 = \mathbf{B}^{(4)^{\mathrm{T}}} \mathbf{D} \varepsilon^{(0)} + \mathbf{B}^{(0)^{\mathrm{T}}} \mathbf{D} \varepsilon^{(4)} + \mathbf{B}^{(1)^{\mathrm{T}}} \mathbf{D} \varepsilon^{(1)}$$
$$\mathbf{a}_5 = \mathbf{B}^{(5)^{\mathrm{T}}} \mathbf{D} \varepsilon^{(0)} + \mathbf{B}^{(0)^{\mathrm{T}}} \mathbf{D} \varepsilon^{(5)} + \mathbf{B}^{(2)^{\mathrm{T}}} \mathbf{D} \varepsilon^{(2)}$$
$$\mathbf{a}_6 = \mathbf{B}^{(3)^{\mathrm{T}}} \mathbf{D} \varepsilon^{(1)} + \mathbf{B}^{(1)^{\mathrm{T}}} \mathbf{D} \varepsilon^{(3)} + \mathbf{B}^{(4)^{\mathrm{T}}} \mathbf{D} \varepsilon^{(2)} + \mathbf{B}^{(2)^{\mathrm{T}}} \mathbf{D} \varepsilon^{(4)}$$
$$\mathbf{a}_7 = \mathbf{B}^{(5)^{\mathrm{T}}} \mathbf{D} \varepsilon^{(1)} + \mathbf{B}^{(1)^{\mathrm{T}}} \mathbf{D} \varepsilon^{(5)} + \mathbf{B}^{(3)^{\mathrm{T}}} \mathbf{D} \varepsilon^{(2)} + \mathbf{B}^{(2)^{\mathrm{T}}} \mathbf{D} \varepsilon^{(3)}$$
$$\mathbf{a}_8 = \mathbf{B}^{(5)^{\mathrm{T}}} \mathbf{D} \varepsilon^{(4)} + \mathbf{B}^{(4)^{\mathrm{T}}} \mathbf{D} \varepsilon^{(5)}$$
$$\mathbf{a}_9 = \mathbf{B}^{(4)^{\mathrm{T}}} \mathbf{D} \varepsilon^{(4)}$$
$$\mathbf{a}_{10} = \mathbf{B}^{(5)^{\mathrm{T}}} \mathbf{D} \varepsilon^{(5)}$$

The tangent stiffness matrix in local system is the second partial derivative of the strain energy U with respect to local variables, it is given as,

$$\mathbf{k}_t = \left[\frac{\partial^2 U}{\partial u_{Lj} \partial u_{Lk}} \right]_{12 \times 12} = \int_V \left(\mathbf{B}^{\mathrm{T}} \mathbf{D} \mathbf{B} + \varepsilon^{\mathrm{T}} \mathbf{D} \frac{\partial \mathbf{B}}{\partial \mathbf{u}_L} \right) \mathrm{d}V \tag{12}$$

where, u_{Lj} and u_{Lk} are the jth and kth components of $\mathbf{u}_L$, respectively. Due to the commutativity of u_{Lj} and u_{Lk} in the differentiation of Eq. (12), $\mathbf{k}_t$ is symmetric.

Equation (12) can be rewritten as

$$\mathbf{k}_t = \int_L \int_A \left(\mathbf{B}^{\mathrm{T}} \mathbf{D} \mathbf{B} + \varepsilon^{\mathrm{T}} \mathbf{D} \frac{\partial \mathbf{B}}{\partial \mathbf{u}_L} \right) \mathrm{d}A \mathrm{d}x$$
$$= \int_L (\mathbf{b}_0 A + \mathbf{b}_1 S_y + \mathbf{b}_2 S_z + \mathbf{b}_3 S_{yz} + \mathbf{b}_4 I_y + \mathbf{b}_5 I_z + \mathbf{b}_6 S_{wyz} + \mathbf{b}_7 S_{wzy} + \mathbf{b}_8 I_{wyz} + \mathbf{b}_9 I_{wy} + \mathbf{b}_{10} I_{wz}) \, \mathrm{d}x$$

where,

$$\mathbf{b}_0 = \mathbf{B}^{(0)^{\mathrm{T}}} \mathbf{D} \mathbf{B}^{(0)} + \varepsilon^{(0)^{\mathrm{T}}} \mathbf{D} \frac{\partial \mathbf{B}^{(0)}}{\partial \mathbf{u}_L}$$
$$\mathbf{b}_1 = \mathbf{B}^{(0)^{\mathrm{T}}} \mathbf{D} \mathbf{B}^{(1)} + \varepsilon^{(0)^{\mathrm{T}}} \mathbf{D} \frac{\partial \mathbf{B}^{(1)}}{\partial \mathbf{u}_L} + \mathbf{B}^{(1)^{\mathrm{T}}} \mathbf{D} \mathbf{B}^{(0)} + \varepsilon^{(1)^{\mathrm{T}}} \mathbf{D} \frac{\partial \mathbf{B}^{(0)}}{\partial \mathbf{u}_L}$$
$$\mathbf{b}_2 = \mathbf{B}^{(0)^{\mathrm{T}}} \mathbf{D} \mathbf{B}^{(2)} + \varepsilon^{(0)^{\mathrm{T}}} \mathbf{D} \frac{\partial \mathbf{B}^{(2)}}{\partial \mathbf{u}_L} + \mathbf{B}^{(2)^{\mathrm{T}}} \mathbf{D} \mathbf{B}^{(0)} + \varepsilon^{(2)^{\mathrm{T}}} \mathbf{D} \frac{\partial \mathbf{B}^{(0)}}{\partial \mathbf{u}_L}$$
$$\mathbf{b}_3 = \mathbf{B}^{(0)^{\mathrm{T}}} \mathbf{D} \mathbf{B}^{(3)} + \varepsilon^{(0)^{\mathrm{T}}} \mathbf{D} \frac{\partial \mathbf{B}^{(3)}}{\partial \mathbf{u}_L} + \mathbf{B}^{(3)^{\mathrm{T}}} \mathbf{D} \mathbf{B}^{(0)} + \varepsilon^{(3)^{\mathrm{T}}} \mathbf{D} \frac{\partial \mathbf{B}^{(0)}}{\partial \mathbf{u}_L} + \mathbf{B}^{(1)^{\mathrm{T}}} \mathbf{D} \mathbf{B}^{(2)} + \varepsilon^{(1)^{\mathrm{T}}} \mathbf{D} \frac{\partial \mathbf{B}^{(2)}}{\partial \mathbf{u}_L} + \mathbf{B}^{(2)^{\mathrm{T}}} \mathbf{D} \mathbf{B}^{(1)} + \varepsilon^{(2)^{\mathrm{T}}} \mathbf{D} \frac{\partial \mathbf{B}^{(1)}}{\partial \mathbf{u}_L}$$
$$\mathbf{b}_4 = \mathbf{B}^{(0)^{\mathrm{T}}} \mathbf{D} \mathbf{B}^{(4)} + \varepsilon^{(0)^{\mathrm{T}}} \mathbf{D} \frac{\partial \mathbf{B}^{(4)}}{\partial \mathbf{u}_L} + \mathbf{B}^{(4)^{\mathrm{T}}} \mathbf{D} \mathbf{B}^{(0)} + \varepsilon^{(4)^{\mathrm{T}}} \mathbf{D} \frac{\partial \mathbf{B}^{(0)}}{\partial \mathbf{u}_L} + \mathbf{B}^{(1)^{\mathrm{T}}} \mathbf{D} \mathbf{B}^{(1)} + \varepsilon^{(1)^{\mathrm{T}}} \mathbf{D} \frac{\partial \mathbf{B}^{(1)}}{\partial \mathbf{u}_L}$$
$$\mathbf{b}_5 = \mathbf{B}^{(0)^{\mathrm{T}}} \mathbf{D} \mathbf{B}^{(5)} + \varepsilon^{(0)^{\mathrm{T}}} \mathbf{D} \frac{\partial \mathbf{B}^{(5)}}{\partial \mathbf{u}_L} + \mathbf{B}^{(5)^{\mathrm{T}}} \mathbf{D} \mathbf{B}^{(0)} + \varepsilon^{(5)^{\mathrm{T}}} \mathbf{D} \frac{\partial \mathbf{B}^{(0)}}{\partial \mathbf{u}_L} + \mathbf{B}^{(2)^{\mathrm{T}}} \mathbf{D} \mathbf{B}^{(2)} + \varepsilon^{(2)^{\mathrm{T}}} \mathbf{D} \frac{\partial \mathbf{B}^{(2)}}{\partial \mathbf{u}_L}$$
$$\mathbf{b}_6 = \mathbf{B}^{(1)^{\mathrm{T}}} \mathbf{D} \mathbf{B}^{(3)} + \varepsilon^{(1)^{\mathrm{T}}} \mathbf{D} \frac{\partial \mathbf{B}^{(3)}}{\partial \mathbf{u}_L} + \mathbf{B}^{(3)^{\mathrm{T}}} \mathbf{D} \mathbf{B}^{(1)} + \varepsilon^{(3)^{\mathrm{T}}} \mathbf{D} \frac{\partial \mathbf{B}^{(1)}}{\partial \mathbf{u}_L} + \mathbf{B}^{(2)^{\mathrm{T}}} \mathbf{D} \mathbf{B}^{(4)} + \varepsilon^{(2)^{\mathrm{T}}} \mathbf{D} \frac{\partial \mathbf{B}^{(4)}}{\partial \mathbf{u}_L} + \mathbf{B}^{(4)^{\mathrm{T}}} \mathbf{D} \mathbf{B}^{(2)} + \varepsilon^{(4)^{\mathrm{T}}} \mathbf{D} \frac{\partial \mathbf{B}^{(2)}}{\partial \mathbf{u}_L}$$
$$\mathbf{b}_7 = \mathbf{B}^{(1)^{\mathrm{T}}} \mathbf{D} \mathbf{B}^{(5)} + \varepsilon^{(1)^{\mathrm{T}}} \mathbf{D} \frac{\partial \mathbf{B}^{(5)}}{\partial \mathbf{u}_L} + \mathbf{B}^{(5)^{\mathrm{T}}} \mathbf{D} \mathbf{B}^{(1)} + \varepsilon^{(5)^{\mathrm{T}}} \mathbf{D} \frac{\partial \mathbf{B}^{(1)}}{\partial \mathbf{u}_L} + \mathbf{B}^{(2)^{\mathrm{T}}} \mathbf{D} \mathbf{B}^{(3)} + \varepsilon^{(2)^{\mathrm{T}}} \mathbf{D} \frac{\partial \mathbf{B}^{(3)}}{\partial \mathbf{u}_L}$$

$$+\mathbf{B}^{(3)^{\mathrm{T}}}\mathbf{D}\mathbf{B}^{(2)}+\varepsilon^{(3)^{\mathrm{T}}}\mathbf{D}\frac{\partial \mathbf{B}^{(2)}}{\partial \mathbf{u}_L}$$

$$\mathbf{b}_8=\mathbf{B}^{(4)^{\mathrm{T}}}\mathbf{D}\mathbf{B}^{(5)}+\varepsilon^{(4)^{\mathrm{T}}}\mathbf{D}\frac{\partial \mathbf{B}^{(5)}}{\partial \mathbf{u}_L}+\mathbf{B}^{(5)^{\mathrm{T}}}\mathbf{D}\mathbf{B}^{(4)}+\varepsilon^{(5)^{\mathrm{T}}}\mathbf{D}\frac{\partial \mathbf{B}^{(4)}}{\partial \mathbf{u}_L}$$

$$\mathbf{b}_9=\mathbf{B}^{(4)^{\mathrm{T}}}\mathbf{D}\mathbf{B}^{(4)}+\varepsilon^{(4)^{\mathrm{T}}}\mathbf{D}\frac{\partial \mathbf{B}^{(4)}}{\partial \mathbf{u}_L}$$

$$\mathbf{b}_{10}=\mathbf{B}^{(5)^{\mathrm{T}}}\mathbf{D}\mathbf{B}^{(5)}+\varepsilon^{(5)^{\mathrm{T}}}\mathbf{D}\frac{\partial \mathbf{B}^{(5)}}{\partial \mathbf{u}_L}$$

Gaussian integral procedure is adopted to calculate the internal force vector and tangent stiffness matrix,

$$\mathbf{f}=\sum_{i=1}^{n_0}\Big[\mathbf{a}_0A+\mathbf{a}_1S_y+\mathbf{a}_2S_z+\mathbf{a}_3S_{yz}+\mathbf{a}_4I_y+\mathbf{a}_5I_z+\mathbf{a}_6S_{wyz}+\mathbf{a}_7S_{wzy}+\mathbf{a}_8I_{wyz}+\mathbf{a}_9I_{wy}+\mathbf{a}_{10}I_{wz}\Big]_{\xi_i}w_t(i)J \tag{13}$$

$$\mathrm{k}_t=\sum_{i=1}^{n_0}\Big[\mathbf{b}_0A+\mathbf{b}_1S_y+\mathbf{b}_2S_z+\mathbf{b}_3S_{yz}+\mathbf{b}_4I_y+\mathbf{b}_5I_z+\mathbf{b}_6S_{wyz}+\mathbf{b}_7S_{wzy}+\mathbf{b}_8I_{wyz}+\mathbf{b}_9I_{wy}+\mathbf{b}_{10}I_{wz}\Big]_{\xi_i}w_t(i)J \tag{14}$$

where, n_0 is the number of Gaussian integral points along the central axis ξ of element, $n_0=2$ in solving the examples below; ξ_i and $w_t(i)$ are the dimensionless coordinate and weight factor at Gaussian point i, respectively; J is the jacobian, $J=\sum_{i=1}^{3}h_i'(\xi)\,x_{i0}$.

The relationship of the global internal force vector $\mathbf{f}_G$ and the local internal force vector $\mathbf{f}$ is given as,

$$\mathbf{f}_G=\mathbf{T}^{\mathrm{T}}\mathbf{f} \tag{15}$$

where, $\mathbf{T}$ is the transformation matrix from global coordinate system to local coordinate system, it is calculated from

$$T_{i,j}=\frac{\partial u_{Li}}{\partial u_{Gj}} \tag{16a}$$

$$\mathbf{T}=\begin{bmatrix}\mathbf{R}&0&0&0&-\mathbf{R}&\mathbf{R}_{16}\\0&\mathbf{R}_{22}&0&0&0&\mathbf{R}_{26}\\0&0&\mathbf{R}&0&-\mathbf{R}&\mathbf{R}_{36}\\0&0&0&\mathbf{R}_{44}&0&\mathbf{R}_{46}\end{bmatrix} \tag{16b}$$

$\mathbf{T}$ is a 12×18 matrix, $\mathbf{R}$ and $\mathbf{R}_{ij}(i=1,2,3,4;j=2,4,6)$ are its sub-matrices. $\mathbf{R}$ represents the same matrix as that in Eq. (5); $\mathbf{R}_{ij}$ is a 3×3 matrix (see Appendix A.1), and '0' is a 3×3 zero matrix.

The global tangent stiffness matrix is derived from $\mathbf{f}_G$ as below,

$$\mathbf{k}_{tG}=\frac{\partial \mathbf{f}_G}{\partial \mathbf{u}_G}=\mathbf{T}^{\mathrm{T}}\frac{\partial \mathbf{f}}{\partial \mathbf{u}_G}+\frac{\partial \mathbf{T}^{\mathrm{T}}}{\partial \mathbf{u}_G}\mathbf{f}=\mathbf{T}^{\mathrm{T}}\mathrm{k}_t\mathbf{T}+\frac{\partial \mathbf{T}^{\mathrm{T}}}{\partial \mathbf{u}_G}\mathbf{f} \tag{17}$$

where, $\mathbf{k}_{tG}$ is an 18×18 matrix; $\frac{\partial \mathbf{T}}{\partial \mathbf{u}_G}$ is a $12\times18\times18$ matrix, it is calculated from

$$\frac{\partial \mathbf{T}}{\partial \mathbf{u}_G}=\begin{bmatrix}\frac{\partial \mathbf{R}}{\partial \mathbf{u}_G}&0&0&0&-\frac{\partial \mathbf{R}}{\partial \mathbf{u}_G}&\frac{\partial \mathbf{R}_{16}}{\partial \mathbf{u}_G}\\0&\frac{\partial \mathbf{R}_{22}}{\partial \mathbf{u}_G}&0&0&0&\frac{\partial \mathbf{R}_{26}}{\partial \mathbf{u}_G}\\0&0&\frac{\partial \mathbf{R}}{\partial \mathbf{u}_G}&0&-\frac{\partial \mathbf{R}}{\partial \mathbf{u}_G}&\frac{\partial \mathbf{R}_{36}}{\partial \mathbf{u}_G}\\0&0&0&\frac{\partial \mathbf{R}_{44}}{\partial \mathbf{u}_G}&0&\frac{\partial \mathbf{R}_{46}}{\partial \mathbf{u}_G}\end{bmatrix} \tag{18}$$

the nonzero sub-matrices of $\frac{\partial \mathbf{R}_{ij}}{\partial \mathbf{u}_G}(i=1,2,3,4;j=2,4,6)$ are given in Appendix A.2. Considering that

$$\frac{\partial \mathbf{T}}{\partial \mathbf{u}_G}=\left[\frac{\partial^2 u_{Li}}{\partial u_{Gj}\partial u_{Gk}}\right]_{12\times18\times18} \tag{19}$$

and the commutativity of the u_{Gj} and u_{Gk} in the differentiation of Eq. (19), it is obvious that the second term in the right-hand side of Eq. (17) is symmetric, furthermore, $\mathbf{k}_{tG}$ is symmetric.

In incremental solution procedure, the equilibrium equation at the start of *ith* loading increment is given as,

$$\mathbf{k}_{tG0}{}^i\Delta\mathbf{u}_{G1}{}^i=\Delta\lambda_1^i\mathbf{P} \tag{20}$$

where, $\mathbf{k}_{tG0}^i$ is the global tangent stiffness matrix at the start of incremental loading Step i; $\Delta\mathbf{u}_{G1}{}^i$ and $\Delta\lambda_1^i$ are the increments of the global variables and the loading parameter, respectively; $\mathbf{P}$ is the prescribed external force vector.

The equilibrium equation at jth iterating step of ith loading increment is given as,

$$\mathbf{k}_{tG}{}_{j-1}^{i}\Delta\mathbf{u}_{G}{}_{j}^{i}=\Delta\lambda_j^i\mathbf{P}+\mathbf{P}_{\mathrm{res}}\quad j\geq2 \tag{21}$$

where, $\mathbf{k}_{tG}{}_{j-1}^{i}$ is the tangent stiffness matrix at the end of $(j-1)$th iterating step; $\Delta\mathbf{u}_{G}{}_{j}^{i}$ and $\Delta\lambda_j^i$ are the increments of the global variables and the loading parameter achieved at jth iterating step; $\mathbf{P}_{\mathrm{res}}$ is the unbalanced loading vector at the end of last iterating step; $\Delta\lambda_1^i$ and $\Delta\lambda_j^i$ are calculated in accordance with general displacement controlling procedure (Yang and Shieh 1990).

For convenience, Eq. (21) can be rewritten as

$$\mathbf{k}_{tG}{}_{j-1}^{i}\mathbf{u}_1{}_j^i=\mathbf{P} \tag{22a}$$

$$\mathbf{k}_{tG}{}_{j-1}^{i}\mathbf{u}_2{}_j^i=\mathbf{P}_{\mathrm{res}} \tag{22b}$$

and the increments of the global variables can be given as

$$\Delta\mathbf{u}_{G}{}_{j}^{i}=\Delta\lambda_j^i\mathbf{u}_1{}_j^i+\mathbf{u}_2{}_j^i \tag{23}$$

Table 1 Comparison of tip displacements under different load levels

Load level (lb)	Tip displacement (in)								
	Present study			Bathe and Bolourchi			Simo and Vu-Quoc		
	u	v	w	u	v	w	u	v	w
300	−7.01	−11.93	−40.15	−6.8	−11.5	−39.5	−6.97	−11.86	−40.08
450	−10.73	−18.47	−48.46	–	–	–	−10.68	−18.38	−48.39
600	−13.55	−23.56	−53.43	−13.4	−23.5	−53.4	−13.51	−23.47	−53.37

Considering that all the global variables are additive in an incremental solution procedure, the global variables at the end of ith loading increment are updated by

$$\mathbf{u}_G^i = \mathbf{u}_G^{i-1} + \sum_{j=1}^{n} \Delta \mathbf{u}_{Gj}^i \tag{24}$$

where, $\mathbf{u}_G^{i-1}$ is the values of the global variables at the end of $(i-1)$th loading increment, and n is the number of iterations at ith increment.

Iterating process will be terminated if the following converge criterion is satisfied,

$$\left| \frac{\mathbf{u}_{2j}^{i\,\mathrm{T}} \mathbf{P}_{\mathrm{res}}}{\Delta \mathbf{u}_{G1}^{i\;\mathrm{T}} \Delta\lambda_1^i \mathbf{P}} \right| \leq \mathrm{err} \tag{25}$$

where, err is a small constant, in analysing the following examples, err $= 10^{-5}$.

5 Examples

5.1 Analysis of a cantilever 45^0-bend with large displacements and large rotations

A bend beam lies in X–Y plane, it is fixed at one end and free at another end (see Fig. 3), a concentrated load is applied at the free end in Z-direction. The bend has an average radius of 100 in, and its cross-section is a square with an area of 1 in^2, and its elastic modulus E and Poisson's ratio μ are 10^7 psi and 0.0, respectively.

This bend is subdivided into eight beam elements equally, and these elements are idealized as straight beams. The tip displacements under different load levels are given in Table 1. To verify the reliability and accuracy of the procedure, the results from Bathe and Bolourchi (1979) and Simo and Vu-Quoc (1986c) are also presented in Table 1, it is shown that the results from present studies can fit in well with them.

In calculating the tip displacements under 600 lb loading level, 8 loading increments are required, and their iteration numbers are 7, 5, 5, 4, 4, 4, 3, 3, respectively.

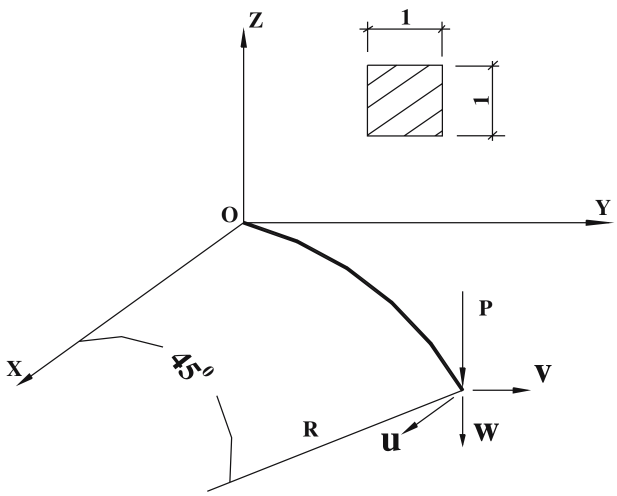

Fig. 3 A cantilever 45^0-bend with a concentrated tip load

5.2 A cantilever subject to an end moment

An initially straight cantilever beam is subjected to an end bending moment $M = 2\pi EI/L$(see Fig. 4), its width and height are $b = 0.5$ and $t = 0.1$, respectively, and its length is 100; its young's modulus is 2.1×10^7, the Poisson's ratio is 0.3, and the cross-sectional shear factor is 5/6.

Considering that the components of nodal external force vector with respect to vectorial rotational variables are not moment in the proposed beam element formulation, the end moment is transformed into equivalent components with respect to vectorial rotational

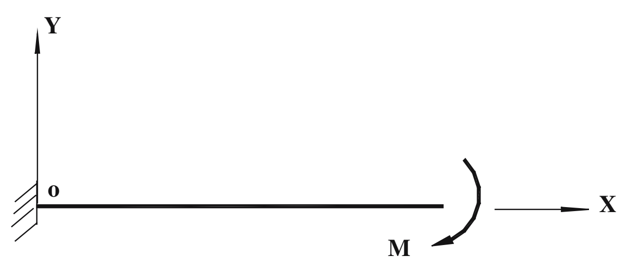

Fig. 4 A cantilever subject to an end moment

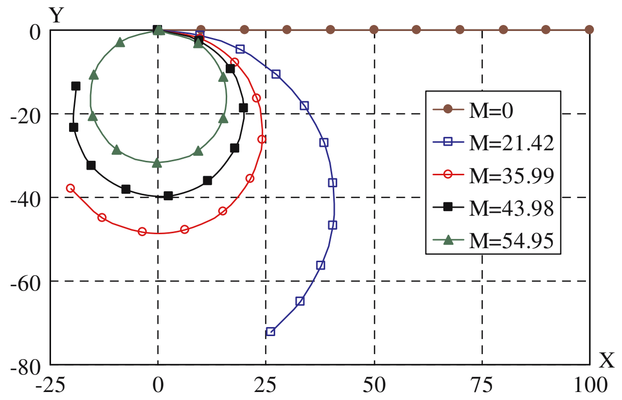

Fig. 5 Deformed shapes of the cantilever under different end moment levels

variables of end node firstly. The relationship of the rotation θ_{iz} and the vectorial rotational variables at end node i is given as below:

If $e_{iy,1} \geq 0$ and $e_{iy,2} > 0$, then $\theta_{iz} = \text{arcsin} e_{iy,1}$;

If $e_{iy,1} < 0$ and $e_{iy,2} > 0$, then $\theta_{iz} = 2\pi + \text{arcsin} e_{iy,1}$;

If $e_{iy,2} \leq 0$, then $\theta_{iz} = \pi - \text{arcsin} e_{iy,1}$.

If $-\frac{\sqrt{2}}{2} \leq e_{iy,1} \leq \frac{\sqrt{2}}{2}$, then $e_{iy,1}$, $e_{iy,3}$ and $e_{iz,1}$ are three vectorial rotational variables at the end node,

$$\delta W = M\delta\theta_{iz} = \frac{M}{e_{iy,2}}\delta e_{iy,1}$$

the equivalent load component with respect to $e_{iy,1}$ is $\frac{M}{e_{iy,2}}$, and another two components with respect to $e_{iy,3}$ and $e_{iz,1}$ are equal to zero.

If $-\frac{\sqrt{2}}{2} < e_{iy,2} < \frac{\sqrt{2}}{2}$, then $e_{iy,2}$, $e_{iy,3}$ and $e_{iz,2}$ are three vectorial rotational variables at the end node,

$$\delta W = M\delta\theta_{iz} = -\frac{M}{e_{iy,1}}\delta e_{iy,2}$$

the equivalent load component with respect to $e_{iy,2}$ is $-\frac{M_i}{e_{iy,1}}$, and another two components with respect to $e_{iy,3}$ and $e_{iz,2}$ are equal to zero.

This cantilever is divided into five beam elements equally. The deformed shapes of the cantilever at different end moment levels are depicted in Fig. 5, it experiences large displacement and large rotation, and its end rotation arrives at 2π under $M = \frac{2\pi EI}{L}$, however, the proposed procedure still demonstrates satisfying efficiency and reliability. Urthaler and Reddy (2005) and Lee (1997) had also solved similar problems (but they did not present the geometry and material properties of the problems), and Lee's procedure (Lee 1997) seems to be quite efficient in solving similar problems, however, it can not cope with buckling and post-buckling problem, and will run into computational difficulty once locking phenomena in thin beam element occur.

5.3 A portal frame subject to a concentrated load

A portal frame is subjected to a concentrated load (see Fig. 6). the cross sections of its three members are rectangular, and their sizes are $b = 0.5$ and $h = 0.1$, respectively. The material properties are $E = 2.1 \times 10^7$ and $\mu = 0.3$, and the cross-sectional shear factor is 5/6.

In order to check the convergence of the proposed procedure, each member is divided into 4, 8 and 16 equal beam elements, respectively. The curve of load against displacement at loading point is depicted in Fig. 7. It is shown that four elements per member are enough to achieve satisfying accuracy. Considering the effects of shear locking and membrane locking phenomena in thin beam element, reduced integration procedure can alleviate or eliminate locking problems of this portal frame effectively.

The deformed shapes of portal frame under different loading levels are depicted in Fig. 8. It demonstrates that the proposed procedure is reliable and efficient in solving large displacement and large rotation problems.

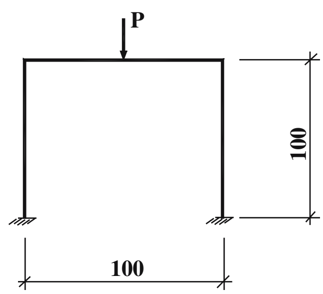

Fig. 6 A portal frame subject to a concentrated load

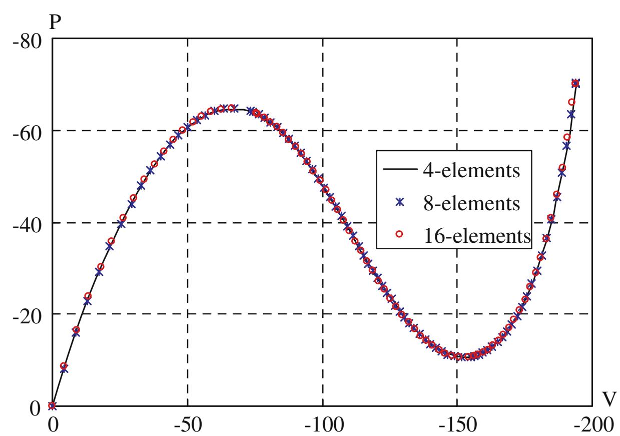

Fig. 7 Response of portal frame subject to a concentrated load

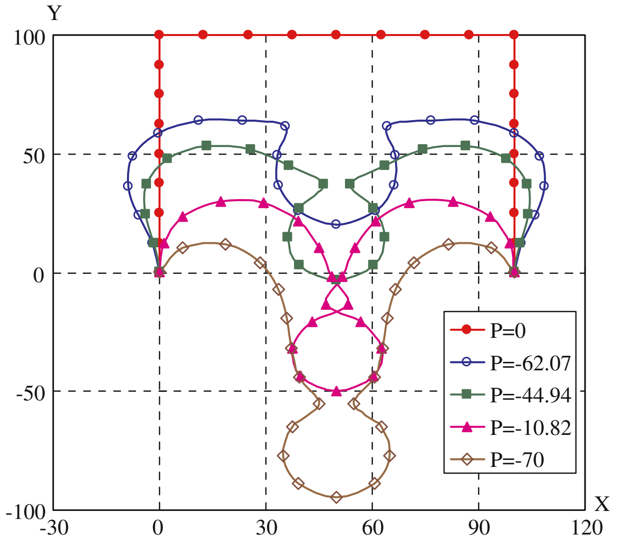

Fig. 8 Deformed shapes of portal frame under different load levels

5.4 Analysis of a space arc frame under vertical and horizontal concentrated loading

This frame is shown in Fig. 9, it consists of two groups of members. For the members in the arc frame planes, the cross-section property are $A_1 = 0.5$, $I_{y1} = 0.4$ and $I_{z1} = 0.133$, respectively, and for the rib members, $A_2 = 0.1$, $I_{y2} = 0.05$ and $I_{z2} = 0.05$, respectively. The material properties are $E = 4.32 \times 10^5$ and $G = 1.66 \times 10^5$. This frame is pinned at four boundary nodes. In addition to four vertical concentrated loads P, the structure is also subjected to two lateral concentrated loads $0.001P$ (see Fig. 9).

In large displacement analysis of this space arc frame, each leg is divided into two equal beam elements, while, the rest members are treated as one element, respectively. The curve of nodal displacement w against load P is given in Fig. 10. It is shown that this curve is in close agreement with the solution given by Hsiao et al. (1987) and Wen and Rahimzadeh (1983).

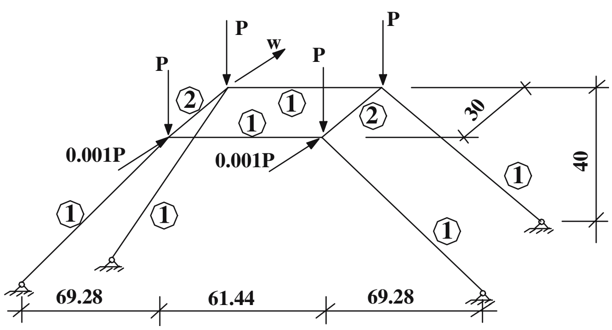

Fig. 9 Space arc frame

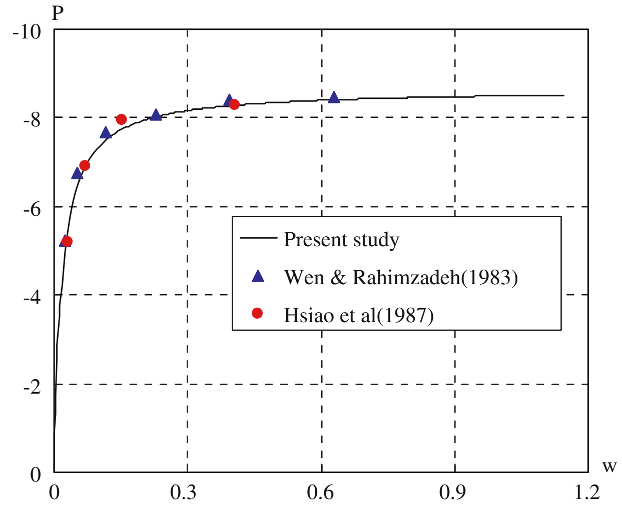

Fig. 10 Response of space arc frame under ultimate concentrated loading

5.5 Space dome subject to a concentrated load at the apex

The space dome is described in Fig. 11, all its members have the same rectangular cross sections, $b \times h = 0.76\,\mathrm{m} \times 1.22\,\mathrm{m}$. The material properties are $E = 2.069 \times 10^{10}$ and $G = 8.83 \times 10^9\,\mathrm{N/m^2}$, respectively. This space

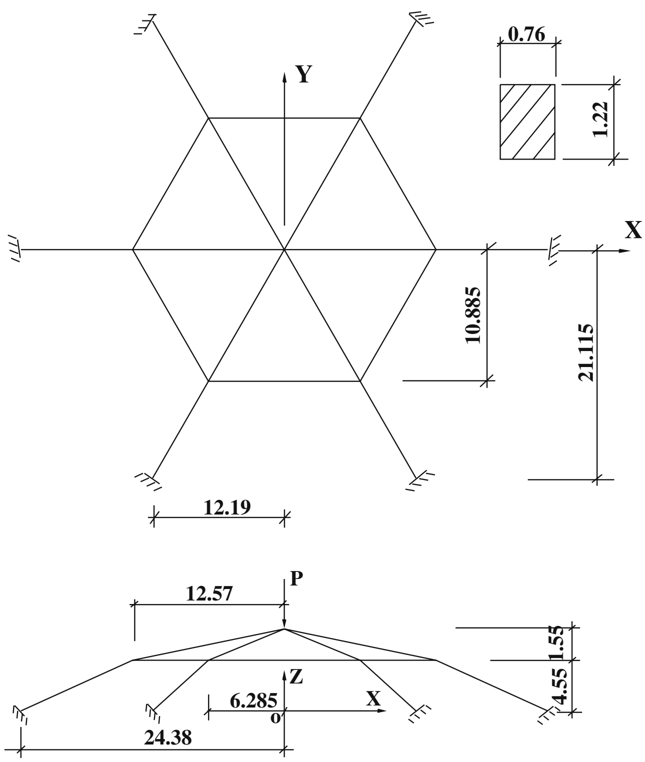

Fig. 11 Geometry of space dome subject to an apex concentrated load

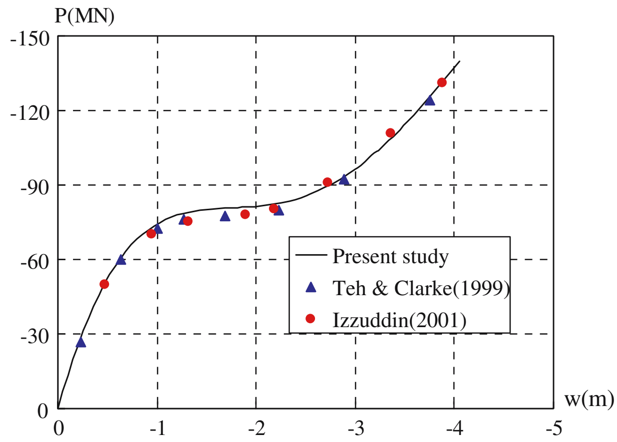

Fig. 12 Load-displacement curve at the peak of space dome

dome is fixed at its six boundary nodes, and a concentrated load is exerted at the apex.

In numerical analysis, each member is modelled by one beam element. The load-displacement curve at the apex is depicted in Fig. 12. Comparison of the results from the proposed procedure and those from Teh and Clarke (1999) and Izzuddin (2001) is given in Fig. 12. It is shown that they are in agreement with each other very well.

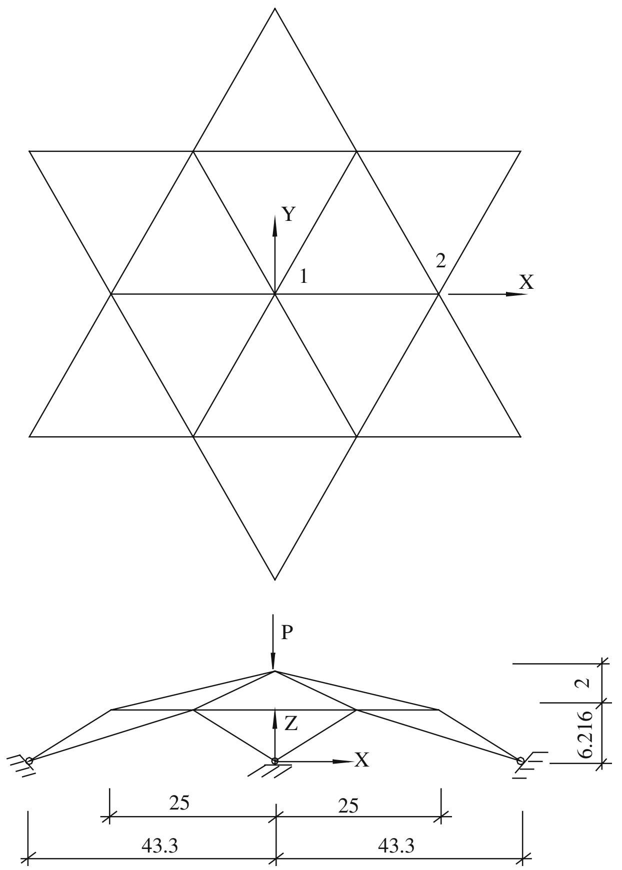

Fig. 13 Twenty four member star-shaped dome subject to a concentrated load at the apex

5.6 Twenty-four-member star-shaped shallow dome

The geometry of a 24-member star-shaped dome is shown in Fig. 13, its member cross-section properties are $A = 3.17\,\text{cm}^2$, $I_y = 0.837\,\text{cm}^4$, $I_z = 0.837\,\text{cm}^4$, and the elastic modulus and shear modulus are $E = 3.03 \times 10^5$ and $G = 1.096 \times 10^5\,\text{N/cm}^2$, respectively. This dome is pinned at six boundary nodes, and is loaded with a concentrated load at the apex.

In numerical analysis of this dome, each member is divided into two equal beam elements. The load-displacement curve of this dome at the apex is depicted in Fig. 14, where the results from Hsiao et al. (1987) and Meek and Tan (1984) are also given, it is shown that the curve from present studies can fit in well with them.

Keeping the same geometry of the dome, the same loading case, and the same material properties and member cross-sectional area, while adjusting the cross section sizes along two principal inertia axes -y and -z: $A = 3.17\,\text{cm}^2$, $I_y = 0.295\,\text{cm}^4$, $I_z = 2.377\,\text{cm}^4$, each member is subdivided into two beam elements equally, the load-displacement curve at the apex is presented in Fig. 15. It illustrates that the response of the dome is greatly different from that in the last case, snap-through phenomenon occurs after the concentrated load arrives at an ultimate level.

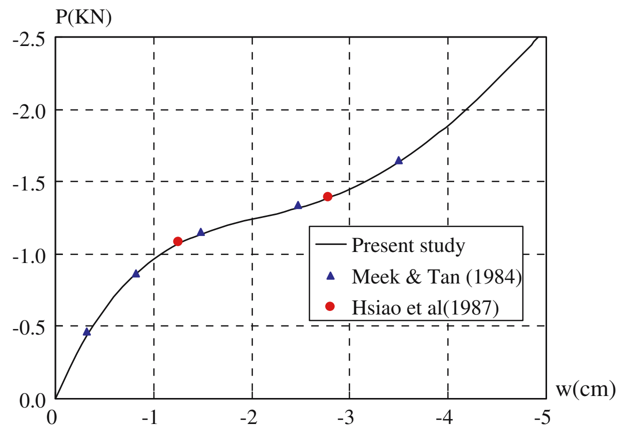

Fig. 14 Load-displacement curve of the star-shaped dome at the apex

The results from Meek and Tan (1984) are also depicted in Fig. 15. Meek and Tan's results are very close to those from present studies.

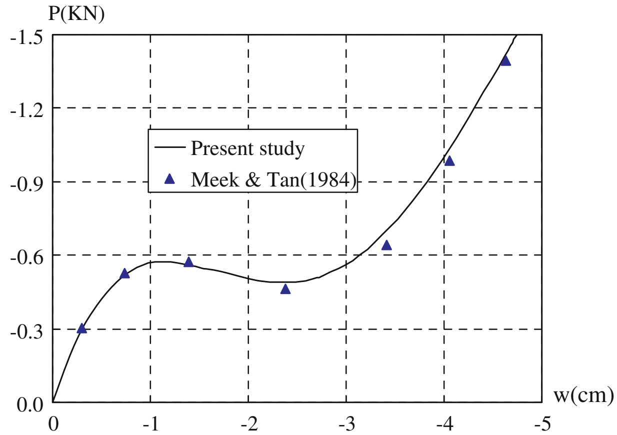

Fig. 15 Load-displacement curve of the dome at the apex

6 Conclusions

Compared with the existing 3-D beam element formulations for frame structures with large displacements and large rotations, there are several advantages in the proposed procedure: (1) the element tangent stiffness matrix is symmetric, so it ensures the computational efficiency and the saving of storage source; (2) vectorial rotational variables are defined so all the variables of freedoms are additive, and 'correction matrix' is avoided; (3) these variables can be used to describe large member deformation. Through several examples test, the proposed procedure demonstrates satisfying accuracy and efficiency in large displacement analyses of frame structures.

where, $i = 1, 3, k = \frac{i+1}{2}$.

$$\mathbf{R}_{i6} = \begin{bmatrix} \left(\frac{\partial \mathbf{R}}{\partial e_{3y,n}} \mathbf{R}_k^{\mathrm{T}} \mathbf{e}_{y0}\right)_{,n_r} & \left(\frac{\partial \mathbf{R}}{\partial e_{3y,m}} \mathbf{R}_k^{\mathrm{T}} \mathbf{e}_{y0}\right)_{,n_r} & \left(\frac{\partial \mathbf{R}}{\partial e_{3z,n}} \mathbf{R}_k^{\mathrm{T}} \mathbf{e}_{y0}\right)_{,n_r} \\ \left(\frac{\partial \mathbf{R}}{\partial e_{3y,n}} \mathbf{R}_k^{\mathrm{T}} \mathbf{e}_{y0}\right)_{,m_r} & \left(\frac{\partial \mathbf{R}}{\partial e_{3y,m}} \mathbf{R}_k^{\mathrm{T}} \mathbf{e}_{y0}\right)_{,m_r} & \left(\frac{\partial \mathbf{R}}{\partial e_{3z,n}} \mathbf{R}_k^{\mathrm{T}} \mathbf{e}_{y0}\right)_{,m_r} \\ \left(\frac{\partial \mathbf{R}}{\partial e_{3y,n}} \mathbf{R}_k^{\mathrm{T}} \mathbf{e}_{z0}\right)_{,n_r} & \left(\frac{\partial \mathbf{R}}{\partial e_{3y,m}} \mathbf{R}_k^{\mathrm{T}} \mathbf{e}_{z0}\right)_{,n_r} & \left(\frac{\partial \mathbf{R}}{\partial e_{3z,n}} \mathbf{R}_k^{\mathrm{T}} \mathbf{e}_{z0}\right)_{,n_r} \end{bmatrix}$$

where, $i = 2, 4, k = \frac{i}{2}$.

$$\mathbf{R}_{(2i)(2i)} = \begin{bmatrix} \left(\mathbf{R} \frac{\partial \mathbf{R}_i^{\mathrm{T}}}{\partial e_{iy,n}} \mathbf{e}_{y0}\right)_{,n_r} & \left(\mathbf{R} \frac{\partial \mathbf{R}_i^{\mathrm{T}}}{\partial e_{iy,m}} \mathbf{e}_{y0}\right)_{,n_r} & \left(\mathbf{R} \frac{\partial \mathbf{R}_i^{\mathrm{T}}}{\partial e_{iz,n}} \mathbf{e}_{y0}\right)_{,n_r} \\ \left(\mathbf{R} \frac{\partial \mathbf{R}_i^{\mathrm{T}}}{\partial e_{iy,n}} \mathbf{e}_{y0}\right)_{,m_r} & \left(\mathbf{R} \frac{\partial \mathbf{R}_i^{\mathrm{T}}}{\partial e_{iy,m}} \mathbf{e}_{y0}\right)_{,m_r} & \left(\mathbf{R} \frac{\partial \mathbf{R}_i^{\mathrm{T}}}{\partial e_{iz,n}} \mathbf{e}_{y0}\right)_{,m_r} \\ \left(\mathbf{R} \frac{\partial \mathbf{R}_i^{\mathrm{T}}}{\partial e_{iy,n}} \mathbf{e}_{z0}\right)_{,n_r} & \left(\mathbf{R} \frac{\partial \mathbf{R}_i^{\mathrm{T}}}{\partial e_{iy,m}} \mathbf{e}_{z0}\right)_{,n_r} & \left(\mathbf{R} \frac{\partial \mathbf{R}_i^{\mathrm{T}}}{\partial e_{iz,n}} \mathbf{e}_{z0}\right)_{,n_r} \end{bmatrix}$$

where, $i = 1, 2$.

Note that the subscripts n_r and m_r denote the $n_r th$ and $m_r th$ components of the related vectors, respectively.

A.2 Sub-matrices of $\frac{\partial \mathbf{T}}{\partial \mathbf{u}_G}$

$$\left.\frac{\partial \mathbf{T}}{\partial \mathbf{u}_G}\right|_{i=i_1:i_3, j=16:18, k=k_1:k_3} = s \left[\frac{\partial \mathbf{R}}{\partial e_{3y,n}} \; \frac{\partial \mathbf{R}}{\partial e_{3y,m}} \; \frac{\partial \mathbf{R}}{\partial e_{3z,n}} \right]$$

where, if $i_1 : i_3 = 1 : 3$ and $k_1 : k_3 = 1 : 3$, or $i_1 : i_3 = 7 : 9$ and $k_1 : k_3 = 7 : 9$, then $s = 1$; if $i_1 : i_3 = 1 : 3$ and $k_1 : k_3 = 13 : 15$, or $i_1 : i_3 = 7 : 9$ and $k_1 : k_3 = 13 : 15$, then $s = -1$. The subscripts at the right side of $\frac{\partial \mathbf{T}}{\partial \mathbf{u}_G}$ represent the location of this sub-matrix in $\frac{\partial \mathbf{T}}{\partial \mathbf{u}_G}$.

$$\left.\frac{\partial \mathbf{T}}{\partial \mathbf{u}_G}\right|_{i=i_1:i_3, j=16:18, k=16:18} = \begin{bmatrix} \frac{\partial^2 \mathbf{R}}{\partial e_{3y,n}^2} (\mathbf{d}_l - \mathbf{d}_3 + \mathbf{v}_{l0}) & \frac{\partial^2 \mathbf{R}}{\partial e_{3y,n} \partial e_{3y,m}} (\mathbf{d}_l - \mathbf{d}_3 + \mathbf{v}_{l0}) & \frac{\partial^2 \mathbf{R}}{\partial e_{3y,n} \partial e_{3z,n}} (\mathbf{d}_l - \mathbf{d}_3 + \mathbf{v}_{l0}) \\ \frac{\partial^2 \mathbf{R}}{\partial e_{3y,n} \partial e_{3y,m}} (\mathbf{d}_l - \mathbf{d}_3 + \mathbf{v}_{l0}) & \frac{\partial^2 \mathbf{R}}{\partial e_{3y,m}^2} (\mathbf{d}_l - \mathbf{d}_3 + \mathbf{v}_{l0}) & \frac{\partial^2 \mathbf{R}}{\partial e_{3y,m} \partial e_{3z,n}} (\mathbf{d}_l - \mathbf{d}_3 + \mathbf{v}_{l0}) \\ \frac{\partial^2 \mathbf{R}}{\partial e_{3y,n} \partial e_{3z,n}} (\mathbf{d}_l - \mathbf{d}_3 + \mathbf{v}_{l0}) & \frac{\partial^2 \mathbf{R}}{\partial e_{3y,m} \partial e_{3z,n}} (\mathbf{d}_l - \mathbf{d}_3 + \mathbf{v}_{k0}) & \frac{\partial^2 \mathbf{R}}{\partial e_{3z,n}^2} (\mathbf{d}_l - \mathbf{d}_3 + \mathbf{v}_{l0}) \end{bmatrix}$$

Appendixes

A. 1 Sub-matrices of $\mathbf{T}$

$$\mathbf{R}_{i6} = \Big[\frac{\partial \mathbf{R}}{\partial e_{3y,n}} (\mathbf{d}_k - \mathbf{d}_3 + \mathbf{v}_{k0}) \; \frac{\partial \mathbf{R}}{\partial e_{3y,m}} (\mathbf{d}_k - \mathbf{d}_3 + \mathbf{v}_{k0}) \; \frac{\partial \mathbf{R}}{\partial e_{3z,n}} (\mathbf{d}_k - \mathbf{d}_3 + \mathbf{v}_{k0}) \Big]$$

where, if $l = 1$, then $i_1 : i_3 = 1 : 3$; if $l = 2$, then $i_1 : i_3 = 7 : 9$.

$$\left.\frac{\partial \mathbf{T}}{\partial \mathbf{u}_G}\right|_{i=i_1:i_3, j=16:18, k=16:18}$$

$$= \begin{bmatrix} \left(\frac{\partial^2 \mathbf{R}}{\partial e_{3y,n}\partial \mathbf{u}_{GS}}\mathbf{R}_l^T\mathbf{e}_{y0}\right)_{,n_r} & \left(\frac{\partial^2 \mathbf{R}}{\partial e_{3y,m}\partial \mathbf{u}_{GS}}\mathbf{R}_l^T\mathbf{e}_{y0}\right)_{,n_r} & \left(\frac{\partial^2 \mathbf{R}}{\partial e_{3z,n}\partial \mathbf{u}_{GS}}\mathbf{R}_l^T\mathbf{e}_{y0}\right)_{,n_r} \\ \left(\frac{\partial^2 \mathbf{R}}{\partial e_{3y,n}\partial \mathbf{u}_{GS}}\mathbf{R}_l^T\mathbf{e}_{y0}\right)_{,m_r} & \left(\frac{\partial^2 \mathbf{R}}{\partial e_{3y,m}\partial \mathbf{u}_{GS}}\mathbf{R}_l^T\mathbf{e}_{y0}\right)_{,m_r} & \left(\frac{\partial^2 \mathbf{R}}{\partial e_{3z,n}\partial \mathbf{u}_{GS}}\mathbf{R}_l^T\mathbf{e}_{y0}\right)_{,m_r} \\ \left(\frac{\partial^2 \mathbf{R}}{\partial e_{3y,n}\partial \mathbf{u}_{GS}}\mathbf{R}_l^T\mathbf{e}_{z0}\right)_{,n_r} & \left(\frac{\partial^2 \mathbf{R}}{\partial e_{3y,m}\partial \mathbf{u}_{GS}}\mathbf{R}_l^T\mathbf{e}_{z0}\right)_{,n_r} & \left(\frac{\partial^2 \mathbf{R}}{\partial e_{3z,n}\partial \mathbf{u}_{GS}}\mathbf{R}_l^T\mathbf{e}_{z0}\right)_{,n_r} \end{bmatrix}$$

where, $\mathbf{u}_{GS} = \{e_{3y,n}, e_{3y,m}, e_{3z,n}\}^T$, if $l = 1$, then $i_1 : i_3 = 4 : 6$; if $l = 2$, then $i_1 : i_3 = 10 : 12$.

$$\left.\frac{\partial \mathbf{T}}{\partial \mathbf{u}_G}\right|_{i=i_1:i_2, j=16:18, k=k_1:k_3} = \left.\frac{\partial \mathbf{T}}{\partial \mathbf{u}_G}\right|_{i=i_1:i_2, k=k_1:k_3, j=16:18}$$

$$= \begin{bmatrix} \left(\frac{\partial \mathbf{R}}{\partial e_{3y,n}}\frac{\partial \mathbf{R}_l^T}{\partial \mathbf{u}_{GS}}\mathbf{e}_{y0}\right)_{,n_r} & \left(\frac{\partial \mathbf{R}}{\partial e_{3y,m}}\frac{\partial \mathbf{R}_l^T}{\partial \mathbf{u}_{GS}}\mathbf{e}_{y0}\right)_{,n_r} & \left(\frac{\partial \mathbf{R}}{\partial e_{3z,n}}\frac{\partial \mathbf{R}_l^T}{\partial \mathbf{u}_{GS}}\mathbf{e}_{y0}\right)_{,n_r} \\ \left(\frac{\partial \mathbf{R}}{\partial e_{3y,n}}\frac{\partial \mathbf{R}_l^T}{\partial \mathbf{u}_{GS}}\mathbf{e}_{y0}\right)_{,m_r} & \left(\frac{\partial \mathbf{R}}{\partial e_{3y,m}}\frac{\partial \mathbf{R}_l^T}{\partial \mathbf{u}_{GS}}\mathbf{e}_{y0}\right)_{,m_r} & \left(\frac{\partial \mathbf{R}}{\partial e_{3z,n}}\frac{\partial \mathbf{R}_l^T}{\partial \mathbf{u}_{GS}}\mathbf{e}_{y0}\right)_{,m_r} \\ \left(\frac{\partial \mathbf{R}}{\partial e_{3y,n}}\frac{\partial \mathbf{R}_l^T}{\partial \mathbf{u}_{GS}}\mathbf{e}_{z0}\right)_{,n_r} & \left(\frac{\partial \mathbf{R}}{\partial e_{3y,m}}\frac{\partial \mathbf{R}_l^T}{\partial \mathbf{u}_{GS}}\mathbf{e}_{z0}\right)_{,n_r} & \left(\frac{\partial \mathbf{R}}{\partial e_{3z,n}}\frac{\partial \mathbf{R}_l^T}{\partial \mathbf{u}_{GS}}\mathbf{e}_{z0}\right)_{,n_r} \end{bmatrix}$$

where, if $l = 1$, then $\mathbf{u}_{GS} = \{e_{1y,n},\ e_{1y,m},\ e_{1z,n}\}^{\mathbf{T}}$, $i_1 : i_3 = 4 : 6$ and $k_1 : k_3 = 4 : 6$; if $l = 2$, then $\mathbf{u}_{GS} = \{e_{2y,n},\ e_{2y,m},\ e_{2z,n}\}^{\mathbf{T}}$, $i_1 : i_3 = 10 : 12$ and $k_1 : k_3 = 10 : 12$.

$$\left.\frac{\partial \mathbf{T}}{\partial \mathbf{u}_G}\right|_{i=i_1:i_3, j=j_1:j_3, k=k_1:k_3}$$

$$= \begin{bmatrix} \left(\mathbf{R}\frac{\partial^2 \mathbf{R}_l{}^T}{\partial e_{ly,n}\partial \mathbf{u}_{GS}}\mathbf{e}_{y0}\right)_{,n_r} & \left(\mathbf{R}\frac{\partial^2 \mathbf{R}_l{}^T}{\partial e_{ly,m}\partial \mathbf{u}_{GS}}\mathbf{e}_{y0}\right)_{,n_r} & \left(\mathbf{R}\frac{\partial^2 \mathbf{R}_l{}^T}{\partial e_{lz,n}\partial \mathbf{u}_{GS}}\mathbf{e}_{y0}\right)_{,n_r} \\ \left(\mathbf{R}\frac{\partial^2 \mathbf{R}_l{}^T}{\partial e_{ly,n}\partial \mathbf{u}_{GS}}\mathbf{e}_{y0}\right)_{,m_r} & \left(\mathbf{R}\frac{\partial^2 \mathbf{R}_l{}^T}{\partial e_{ly,m}\partial \mathbf{u}_{GS}}\mathbf{e}_{y0}\right)_{,m_r} & \left(\mathbf{R}\frac{\partial^2 \mathbf{R}_l{}^T}{\partial e_{lz,n}\partial \mathbf{u}_{GS}}\mathbf{e}_{y0}\right)_{,m_r} \\ \left(\mathbf{R}\frac{\partial^2 \mathbf{R}_l{}^T}{\partial e_{ly,n}\partial \mathbf{u}_{GS}}\mathbf{e}_{z0}\right)_{,n_r} & \left(\mathbf{R}\frac{\partial^2 \mathbf{R}_l{}^T}{\partial e_{ly,m}\partial \mathbf{u}_{GS}}\mathbf{e}_{z0}\right)_{,n_r} & \left(\mathbf{R}\frac{\partial^2 \mathbf{R}_l{}^T}{\partial e_{lz,n}\partial \mathbf{u}_{GS}}\mathbf{e}_{z0}\right)_{,n_r} \end{bmatrix}$$

where, if $l = 1$, then $\mathbf{u}_{GS} = \{e_{1y,n},\ e_{1y,m},\ e_{1z,n}\}^T$, $i_1 : i_3 = 4 : 6$, $j_1 : j_3 = 4 : 6$ and $k_1 : k_3 = 4 : 6$; if $l = 2$, then $\mathbf{u}_{GS} = \{e_{2y,n},\ e_{2y,m},\ e_{2z,n}\}^T$, $i_1 : i_3 = 10 : 12$, $j_1 : j_3 = 10 : 12$ and $k_1 : k_3 = 10 : 12$.

References

Bathe KJ, Bolourchi S (1979) Large displacement analysis of three-dimensional beam structures. Int J Numer Methods Eng 14:961–986

Battini JM, Pacoste C (2002) Co-rotational beam elements with warping effects in instability problems. Comput Methods Appl Mech Eng 191:1755–1789

Cardona A, Geradin M (1988) Beam finite element non-linear theory with finite rotations. Int J Numer Methods Eng 26:2403–2438

Chen H, Blandford GE (1991) Thin-walled space frames. I. Large-deformation analysis theory. J Struct Eng ASCE 117:2499–2520

Crisfield MA (1990) Consistent co-rotational formulation for non-linear, three-dimensional, beam-elements. Comput Methods Appl Mech Eng 81:131–150

Crisfield MA (1996) Nonlinear finite element analysis of solid and structures, vol 2. Wiley, Chichester

Crisfield MA, Moita GF (1996) A unified co-rotational framework for solids, shells and beams. Int J Solids Struct 33:2969–2992

Hsiao KM, Horng HJ, Chen YR (1987) A co-rotational procedure that handles large rotations of spatial beam structures. Comput Struct 27:769–781

Hsiao KM, Lin WY (2000a) A co-rotational finite element formulation for buckling and postbuckling analyses of spatial beams. Comput Methods Appl Mech Eng 188:567–594

Hsiao KM, Lin WY (2000b) Co-rotational formulation for thin-walled beams with monosymmetric open section. Comput Methods Appl Mech Eng 190:1163–1185

Izzuddin BA (2001) Conceptual issues in geometrically nonlinear analysis of 3D framed structures. Comput methods Appl Mech Eng 191:1029–1053

Izzuddin BA, LI Z (2004) A co-rotational formulation for large displacement analysis of curved shell. In: Deeks, Hao (eds) The 18th Australasian conference on the mechanics of structures & materials. Taylor & Francis Group, London, pp 1247–1253

Jiang L, Chernuka MW (1994) Co-rotational formulation for geometrically nonlinear finite element analysis of spatial beams. Trans Can Soc Mech Eng 18:65–88

Kwak HG, Kim DY, Lee HW (2001) Effect of warping in geometric nonlinear analysis of spatial beams. J Construct Steel Res 57:729–751

Lee K (1997) Analysis of large displacements and large rotations of three-dimensional beams by using small strains and unit vectors. Commun Numer Methods Eng 13:987–997

Li ZX, Izzuddin BA (2005) Application of vectorial rotational variables in large displacement analysis of structures. In: Shen ZY, Li GQ, Chan SL (eds) The fourth international conference on advances in steel structures. Elsevier, Oxford, pp 1501–1506

Lin WY, Hsiao KM (2001) Co-rotational formulation for geometric nonlinear analysis of doubly symmetric thin-walled beams. Comput Methods Appl Mech Eng 190:6023–6052

Meek JL, Tan HS (1984) Geometrically nonlinear analysis of space frames by an incremental iterative technique. Comput Methods Appl Mech Eng 47:261–282

Misra A, Behdinan K, Cleghorn WL (2000) Implementation of consistent updated Lagrangian formulation for static analysis of geometrically nonlinear beam. Trans Can Soc Mech Eng 24:135–142

Pai PF, Anderson TJ, Wheater EA (2000) Large-deformation tests and total-Lagrangian finite-element analyses of flexible beams. Int J Solids Struct 37:2951–2980

Schulz M, Filippou FC (2001) Non-linear spatial timoshenko beam element with curvature interpolation. Int J Numer Methods Eng 50:761–785

Simo JC (1992) (Symmetric) Hessian for geometrically nonlinear models in solid mechanics. Intrinsic definition and geometric interpretation. Comput Methods Appl Mech Eng 96:189–200

Simo JC, Vu-Quoc L (1986a) On the dynamics of flexible beams under large overall motions – the plane case: part I. J Appl Mech ASME 53:849–854

Simo JC, Vu-Quoc L (1986b) On the dynamics of flexible beams under large overall motions – the plane case: part II. J Appl Mech ASME 53:855–863
Simo JC, Vu-Quoc L (1986c) A three-dimensional finite-strain rod model. Part II: computational aspects. Comput Methods Appl Mech Eng 58:79–116
Simo JC, Vu-Quoc L (1988) On the dynamics in space of rods undergoing large motions – a geometrically exact approach. Comput Methods Appl Mech Eng 66:125–161
Simo JC, Vu-Quoc L (1991) A geometrically-exact rod model incorporating shear and torsion-warping deformation. Int J Solids Struct 27:371–393
Teh LH, Clarke MJ (1998) Co-rotational and Lagrangian formulations for elastic three-dimensional beam finite elements. J Construct Steel Res 48:123–144
Teh LH, Clarke MJ (1999) Symmetry of tangent stiffness matrices of 3D elastic frame. J Eng Mech ASCE 125:248–251
Urthaler Y, Reddy JN (2005) A corotational finite element formulation for the analysis of planar beams. Commun Numer Methods Eng 21:553–570
Vu-Quoc L, Deng H (1995) Galerkin projection for geometrically exact sandwich beams allowing for ply drop-off. J Appl Mech ASME 62:479–488
Vu-Quoc L, Ebcioglu IK (1995) Dynamic formulation for geometrically-exact sandwich beam and 1-plates. J Appl Mech ASME 62:756–763
Vu-Quoc L, Ebcioglu IK (1996) General multilayer geometrically-exact beams and 1-D plates with piecewise linear section deformation. Zeitschrift fuer Angewandte Math Mech 76:391–409
Vu-Quoc L, Simo JC (1987) Dynamics of earth-orbiting flexile satellites with multibody components. J Guid Control Dyn 10:549–558
Wen RK, Rahimzadeh J (1983) Nonlinear elastic frame analysis by finite element. J Struct Eng ASCE 109:1951–1971
Yang YB, Shieh MS (1990) Solution method for nonlinear problems with multiple critical points. AIAA J 28:2110–2116